



Published in final edited form as:

Heart Rhythm. 2016 August ; 13(8): 1716–1723. doi:10.1016/j.hrthm.2016.05.009.

Arrhythmogenic Calmodulin Mutations Impede Activation of Small-conductance Calcium-Activated Potassium Current

Chih-Chieh Yu, MD^{1,2}, Jum-Suk Ko, MD, PhD^{1,3}, Tomohiko Ai, MD, PhD^{1,4}, Wen-Chin Tsai, MD^{1,5}, Zhenhui Chen, PhD¹, Michael Rubart, MD^{1,6}, Matteo Vatta, PhD^{1,7}, Thomas H. Everett, IV, PhD.¹, Alfred L. George Jr., MD⁸, and Peng-Sheng Chen, MD, FHRS¹

¹Krannert Institute of Cardiology and Division of Cardiology, Department of Medicine, Indiana University, Indianapolis, IN

²Department of Internal Medicine, National Taiwan University Hospital, Taipei, Taiwan

³Division of Cardiology, Department of internal medicine, Wonkwang University School of Medicine and Hospital, Iksan, Korea

⁴Department of Molecular Pathogenesis, Medical Research Institute; the Department of Emergency Medicine, Tokyo Medical and Dental University

⁵Hualein Tzu-Chi General Hospital, Taiwan

⁶Department of Pediatrics, Riley Heart Research Center, Chicago, IL

⁷Department of Medical and Molecular Genetics, Indiana University School of Medicine, Chicago, IL

⁸Department of Pharmacology, Northwestern University Feinberg School of Medicine, Chicago, IL

Abstract

Background—Apamin sensitive small-conductance Ca^{2+} -activated K^+ (SK) channels are gated by intracellular Ca^{2+} through a constitutive interaction with calmodulin.

Objective—We hypothesize that arrhythmogenic human calmodulin mutations impede activation of SK channels.

Methods—We studied 5 previously published calmodulin mutations (N54I, N98S, D96V, D130G and F90L). Plasmids encoding either wild type (WT) or mutant calmodulin were transiently transfected into human embryonic kidney (HEK) 293 cells that stably express SK2 channels (SK2 Cells). Whole-cell voltage-clamp recording was used to determine apamin-sensitive current (I_{KAS}) densities. We also performed optical mapping studies in normal murine

Corresponding Author: Peng-Sheng Chen, MD, 1800 N. Capitol Ave, Room E475, Indianapolis, IN 46202-1228 Telephone: (317) 274-0909, Fax: (317) 962-0588, chenpp@iu.edu.

Publisher's Disclaimer: This is a PDF file of an unedited manuscript that has been accepted for publication. As a service to our customers we are providing this early version of the manuscript. The manuscript will undergo copyediting, typesetting, and review of the resulting proof before it is published in its final citable form. Please note that during the production process errors may be discovered which could affect the content, and all legal disclaimers that apply to the journal pertain.

Disclosures: Dr Peng-Sheng Chen has equity interest in Arrhythmotech, LLC. Our laboratory receives equipment donations from Medtronic, St Jude and Cyberonics Inc. Dr. George receives research grants from Gilead Sciences, Inc. and Merck, Inc.

hearts to determine the effects of apamin in hearts with (N=7) or without (N=3) pretreatment with sea anemone toxin (ATX II).

Results—SK2 cells transfected with WT calmodulin exhibited I_{KAS} density (in pA/pF) of 33.6 [31.4;36.5] (median and confidence interval 25%-75%), significantly higher than that observed for cells transfected with N54I (17.0 [14.0;27.7], $p=0.016$), F90L (22.6 [20.3;24.3], $p=0.011$), D96V (13.0 [10.9;15.8], $p=0.003$), N98S (13.7 [8.8;20.4], $p=0.005$) and D130G (17.6 [13.8;24.6], $p=0.003$). The reduction of SK2 current was not associated with a decrease in membrane protein expression or intracellular distribution of the channel protein. Apamin increased the ventricular APD₈₀ (from 79.6 ms [63.4-93.3] to 121.8 ms [97.9-127.2], $p=0.010$) in hearts pre-treated with ATX-II but not in control hearts.

Conclusion—Human arrhythmogenic calmodulin mutations impede the activation of SK2 channels in HEK 293 cells.

Keywords

Long QT syndrome; catecholaminergic polymorphic ventricular tachycardia; ion channels; cardiac electrophysiology; arrhythmias

Introduction

Small conductance calcium-activated potassium (SK) channels carry a repolarization current responsible for afterhyperpolarization of neurons in the nervous system and contributes to the modulation of intrinsic excitability, synaptic transmission and long-term changes that affect learning and memory formation.^{1, 2} SK also contributes significantly to the repolarization of atrial myocytes^{3, 4} and promotes automaticity and atrioventricular node conduction.⁵ SK is upregulated in atrial fibrillation, heart failure and myocardial infarction.^{4, 6-8} While SK current is difficult to detect in normal ventricular myocytes at normal pacing rates,^{3, 6, 9} it is important for ventricular repolarization during bradycardia and atrioventricular (AV) block.¹⁰ Apamin is a specific SK current blocker in both neuronal type and cardiac type ion channels.^{1, 11} SK current blockade by apamin can cause premature ventricular contraction, QT prolongation and torsades de pointes ventricular arrhythmia in normal rabbit ventricles.¹⁰ However, there are no reported cases of SK channel mutations in humans with cardiac arrhythmias. Therefore, the importance of SK current in human arrhythmogenesis remains unclear. Calmodulin mutations were reported to be associated with catecholaminergic polymorphic ventricular tachycardia (CPVT; N54I, N98S),¹² congenital long QT syndrome (LQTS) with recurrent cardiac arrest (D96V, D130G and F142L)¹³ and childhood and adolescent onset idiopathic ventricular fibrillation (VF) (F90L).¹⁴ Because SK channels are gated by intracellular Ca^{2+} through a constitutive interaction between the pore-forming subunits and calmodulin,¹ it is possible that mutant calmodulin may impede the activation of the SK currents. We used human embryonic kidney (HEK) 293 cells that stably express subtype 2 of SK protein (SK2 cells) to test this hypothesis.

Methods

The study was approved by the Institutional Biosafety Committee and Institutional Animal Care and Use Committee of the Indiana University and the Methodist Research Institute, Indianapolis, Indiana. Detailed methods are included in an online supplement.

Transfection of wild type and mutant calmodulins

SK2 cells were transfected with various plasmids. The amount of wild type calmodulin plasmids (WT-CaM/pIRES2-EGFP or WT-CaM/pIRES2-dsRED) or mutant calmodulin plasmids (N54I, F90L, D96V, N98S, D130G/pIRES2-EGFP) transfected was either 1 μg each or 1 μg total in combination (for co-expression experiments).

Patch-clamp experiments

Whole cell voltage-clamp technique was performed.¹¹ The Tyrode's (bath) solution contains (in mM) NaCl 140, KCl 5.4, MgCl_2 1.2, HEPES 5, NaH_2PO_4 0.33, CaCl_2 1.8 and D-glucose 10 (pH 7.4 adjusted with NaOH). The pipette solution contained (in mM) K-Gluconate 144, MgCl_2 1.15, EGTA 1, HEPES 10 and different concentration of CaCl_2 (pH 7.2 adjusted with KOH). Free Ca^{2+} concentration was 1.0 $\mu\text{mol/L}$ for all experiments except when testing calcium sensitivities (0.1 to 10 μM). All experiments were carried out at 37°C. SK2 current density was calculated as the difference of current at 0 mV before and after exposure to apamin (500 nM).

Immunofluorescence imaging

HEK 293 cells and SK2 cells were seeded and grown on coated glass coverslips. The cells were stained with anti-SK2 rabbit polyclonal antibody, incubated with Alexa Fluor 568 goat anti-rabbit IgG secondary and counterstained with DAPI. The cover glasses were then mounted onto a glass slide and imaged by a Leica TCS SP8 laser scanning confocal microscope. To minimize variability, we plated cells on the same day, introduced plasmids in the same way and immunostained all samples altogether. We used the same imaging conditions and acquired images within 2~3 hours to reduce photobleaching. We then compared cells side by side in the same region in the same sample.

Western blot analysis

HEK 293 cells and SK2 cells were washed in cold PBS and subsequently lysed and homogenized in 10 mM cold sodium bicarbonate. The membrane fractions were harvested by centrifugation. The protein concentrations were measured with Lowry protein assay. Sixty μg of microsomes were subjected to a SDS-polyacrylamide gel electrophoresis and transferred to a nitrocellulose membrane. The blot was probed with a rabbit anti-SK2 polyclonal antibody. Antibody-bound protein bands were visualized with 125I-protein A followed by autoradiography. The membrane was then scanned in a flat-bed scanner at 600 dpi and the staining densities were analyzed using ImageJ 1.49b.

Optical mapping studies

We used 10 wild type (WT) mice for optical mapping of membrane potential. The hearts were Langendorff perfused with 37°C oxygenated Tyrode's solution and stained with dye di-4-ANEPPS. Blebbistatin (10 mM) was added to the Tyrode's solution. Hearts were illuminated with a solid-state laser. Seven hearts were first treated with 15 nM sea anemone toxin (ATX-II) to prolong QT interval, followed by 100 nM of apamin. The remaining 3 hearts were treated with 100 nM of apamin only. The action potential duration measured to 80% repolarization (APD₈₀) was determined at pacing cycle lengths (PCL) of 200 ms.

Statistical analysis

Data in text and figures are presented as median and confidence interval [25th percentile; 75th percentile] except the figure of normalized calcium sensitivity curve which is presented as mean ± standard error. Nonparametric tests were used for data analyses. Mann-Whitney U test was conducted to compare SK2 current densities between groups with or without transfected calmodulins. Kruskal-Wallis test was performed to test the existence of a statistically significant difference among mutant calmodulins. Repeated measures analyses of variance (RMANOVA) was used to compare the effects of WT:D96V ratio on current density and APD changes in the optical mapping studies. A *p* value < 0.05 was considered statistically significant. Statistical analyses were performed using SPSS (IBM, Chicago, IL, USA, version 21).

Results

Figure 1A illustrates representative current tracings from an SK2 cell before (trace a) and after (trace b) apamin, respectively, obtained by the descending voltage ramp protocol shown in the inset. Trace b shows the small endogenous current (<100 pA). Figure 1B shows the time course of the entire experiment. The current was fully activated 4 min after break-in and was completely suppressed by apamin. In Figure 1C, immunofluorescence shows SK2 protein (red fluorescence) expressed in all SK2 cells (left panel) while no detectable SK2 fluorescence was observed in naïve HEK 293 cells (right panel). This examination also confirmed the specificity of the SK2 antibody in HEK 293 cells.

Overexpression of wild type calmodulin increases SK2 current densities

Figure 2 shows a summary of SK2 current densities (i) in SK2 cells expressing one of 5 mutant calmodulins or wild type calmodulin (WT-calmodulin), (ii) in SK2 cells transfected with GFP only, (iii) in SK2 cells without transfection and (iv) in naïve HEK 293 cells. The median current density of SK2 cells was 14.1 pA/pF [12.0;24.3], significantly higher than that of naïve HEK 293 cells, 0.16 pA/pF [0.07;0.18] (*p*=0.011). The SK2 current densities of SK2 cells transfected with GFP plasmids only (18.33 pA/pF [8.0;23.4]) were not significantly different from that in SK2 cells (*p*=0.806). When SK2 cells were transfected with wild type calmodulin, the current densities significantly increased to 33.6 pA/pF [31.4;36.5] (*p*=0.005 compared to SK2 cells transfected with GFP).

Mutant calmodulins reduce SK2 current densities compared to wild type calmodulin

We then determined the SK2 current densities of the cells transfected with mutant calmodulins. Compared with the cells transfected with WT calmodulin, the median SK2 current density in cells transfected with mutant calmodulins was significantly reduced: N54I (17.0 pA/pF [14.0;27.7], $p=0.016$), F90L (22.6 pA/pF [20.3;24.3], $p=0.011$), D96V (13.0 pA/pF [10.9;15.8], $p=0.003$), N98S (13.7 pA/pF [8.8;20.4], $p=0.005$) and D130G (17.6 pA/pF [13.8;24.6], $p=0.003$). There were no significant differences in median current density among SK2 cells expressing mutant calmodulins ($p=0.273$) nor between SK2 cells expressing a mutant calmodulin and untransfected SK2 cells. These findings were consistent with loss-of-function calmodulin mutations.

To examine the possibility that calmodulin mutants exert a dominant-negative effect on SK2 currents, we next measured SK2 currents in SK2 cells co-transfected with varying ratios of WT and D96V mutant calmodulin. The results of these measurements are summarized in Figure 3. A gradual increase in the proportion of D96V calmodulin plasmid caused a progressive decrease in SK2 current density ($p<0.05$). We also found that the SK2 current density measured in SK2 cells transfected with 0.5 μ g WT calmodulin was not significantly different from the SK2 current density in cells co-transfected with the same amount of WT and D96V plasmid each, suggesting that the D96V mutant calmodulin lacked a dominant-negative effect on endogenous WT calmodulin. However, whether mutant calmodulin competes with WT calmodulin for interaction with the SK channel itself remains unclear.

Ca sensitivity of D96V

Figure 4 shows a calcium sensitivity curve for SK2 current measured in the presence of either WT or D96V calmodulin. The reduction of SK2 current density was observed at all intracellular calcium concentrations. The K_d of D96V was 0.36 ± 0.07 μ M, significantly lower than that of WT-calmodulin, 0.82 ± 0.13 μ M ($p=0.018$), implying a relatively higher Ca sensitivity of SK2 current in the SK2 cells transfected with D96V calmodulin. The Hill coefficients were not significantly different between D96V and WT-calmodulin (6.21 ± 3.07 vs. 3.48 ± 1.91 , $p=0.662$). The reason why a mutant calmodulin (D96V) that greatly reduced Ca^{2+} binding affinity caused enhanced Ca^{2+} -affinity to activate SK current remained unclear.

Mutant calmodulins do not affect SK2 cell surface expression

To investigate the underlying mechanisms, we performed confocal microscopy studies to determine intracellular SK2 protein distribution in the presence of mutant and WT calmodulins (Figure 5). Green fluorescence marked SK2 cells successfully transfected with calmodulin whereas red fluorescence indicated expression of SK2 protein. The nuclei were stained blue with DAPI. Neither extrinsic WT-calmodulin nor extrinsic mutant calmodulins had apparent effects on intracellular SK2 protein distribution. There were similar amounts of SK2 protein expression in GFP (+) and GFP (-) cells.

Next, we used western blot analysis to study if the SK2 protein expression was altered by co-expression of calmodulin in the HEK 293 cells (Figure 6, $n=3$). While there was no detectable SK2 protein in untransfected HEK 293 cells, all SK2 cells expressed SK2 protein. There were no significant differences of SK2 protein production among SK2 cells

transfected with WT or mutant calmodulin. Whether mutant calmodulins suppressed SK current by limiting channel trafficking to the plasma membrane was not determined.

Relevance of SK current in long QT syndrome

We showed that apamin alone did not prolong the action potential duration (APD) (46.5 ms [45.8:47.7]) as compared with baseline (47.2 ms [46.3:48.2], $p=0.120$). However, in murine hearts pretreated with ATX-II to create a model of long QT syndrome,^{15, 16} apamin further prolonged the APD. With pacing cycle length of 200 ms, the APD was 52.0 ms [39.7-53.1] at baseline, 79.6 ms [63.4:93.3] after ATX-II and 121.8 ms [97.9-127.2] after ATX-II + apamin ($p=0.001$; Figure 7). These data indicate that suppression of SK current can potentiate the long QT phenotype.

Discussion

Co-expression of WT calmodulin significantly enhanced the current density of the SK2 cells, while mutant calmodulin abolished this effect. The cotransfection of WT and D96V calmodulins in cultured HEK 293 cells caused a dose-dependent loss-of-function in SK2 gating, suggesting haploinsufficiency as its mechanism. The effect of D96V on SK2 gating is probably induced by a failure of the mutated calmodulin to fully open SK2 channels in response to elevated intracellular calcium.

Calmodulin is a limiting factor in SK2 current regulation

The significant increase of SK2 current when SK2 cells are transiently transfected with WT calmodulin implies that the amount of WT calmodulin in the cell is a limiting factor of SK2 current activation. Calmodulin had been shown to be a limiting factor in both naïve HEK 293 cells and cardiomyocytes.¹⁷⁻²⁰ In a series of studies using Fluorescent Resonance Energy Transfer (FRET)-based biosensors to investigate the dynamic changes of free calmodulin in HEK 293 cells, the available free apo- and calcified calmodulin concentration in the resting state was 8.8 μM , and it fell below the detectable limit for the biosensor when the free calcium concentration reached $\sim 4 \mu\text{M}$. Under this condition, almost all of the calmodulin became bound and not available. These findings indicate an overall excess of calmodulin-binding sites in the HEK 293 cells.^{17, 18} Similar results were later obtained in rabbit ventricular myocyte studies that showed only 1% (50-75 nM) of total calmodulin (6 μM) was available at resting (100-150 nM) Ca^{2+} concentration, suggesting intense competition of targets for free calmodulin.^{19, 20} With only $\sim 1\%$ free calmodulin available in the cell, most calmodulin targets are likely to require pre-bound calmodulin for effective signaling.²¹ Because SK channels are constitutively bound to calmodulin,¹ they are likely to operate through the same mechanism.

D96V mutation results in loss-of-function calmodulin and impedes SK2 activities

When SK2 channels are produced and traffic to the cell membrane, calmodulin is already constitutively bound to the calmodulin binding domain (CaMBD) of SK2 channel.^{22, 23} The C-lobe of calmodulin is bound to SK2 CaMBD in a Ca^{2+} -independent manner and this interaction is also required for surface expression of SK channels.²³⁻²⁶ The N-lobe of calmodulin is important for mediating SK channel gating by binding Ca^{2+} to the EF hand

motifs.^{23, 26} In in-vitro studies, the Ca²⁺ affinity of C-domain of D96V, N98S, F142L and D130G calmodulins was reduced, while Ca²⁺ affinity of N-domains was not changed compared to wild type.^{13, 27} However, in the SK2 channel complex, calmodulin is constitutively bound to the CaMBD of SK2 channel via C-domain of calmodulin. We do not know whether these mutations would hinder or enhance the binding between calmodulin and SK2 channels. A crystal structure study showed that the C-domain of the calmodulin in the SK2 channel complex was conformationally distinct from Ca²⁺-bound status in vitro.²³ Similarly, it is also not known whether the Ca affinity of N-domain in vitro represents the Ca affinity of N-domain when the C-domain is already bound on CaMBD of SK2 channel and already experiences conformational change. Therefore, the data from recently published in vitro Ca binding assay may not be directly relevant to our study. It is reasonable to hypothesize that the mutations of the C-lobe may hinder the binding of calmodulin onto SK2 channel or impede the trafficking of SK2 protein onto cell membrane. Our confocal immunofluorescence experiments showed similar pattern of intracellular distribution of SK2 protein among SK2 cells with or without WT or mutant calmodulin transfection. These findings imply that SK2 protein distribution is not affected by excess amount of calmodulin expression nor the presence of mutated calmodulin.

In the WT:D96V cotransfection study (figure 3), there was a progressive decrease in the SK current density with an increasing D96V:WT ratio, suggesting that D96V calmodulin lost its function on gating SK2 channel. The left shift of Ca-sensitivity curve of D96V indicates increased Ca²⁺ sensitivity (figure 4B). In vitro Ca²⁺ binding studies¹³ showed D96V reduced Ca²⁺ affinity in the C-domain but not in the N-domain. We postulate that, at lower total Ca²⁺ concentration, the reduced Ca²⁺ binding affinity of C domain (of D96V calmodulin) increases the availability of intracellular free Ca²⁺ for the EF hands in the N-lobe of calmodulin, which results in conformational changes that increased Ca²⁺-sensitivity of the SK2 current. The same mechanism does not operate at higher Ca²⁺ concentration (1 μ M or higher), when Ca²⁺ is easily available to both N and C terminal domains.

Because of the existence of intrinsic calmodulin in D96V transfected SK2 cells, each SK2 channel would be composed of different proportions of WT and mutant calmodulins. Our findings suggest that co-existence of D96V calmodulins in each SK2 channel complex increased SK2 channel Ca²⁺ sensitivity. In patients harboring heterozygous calmodulin mutations, we may expect the same mechanism with the SK2 current more easily activated, but producing a subnormal SK2 current in a cardiomyocyte or a neuron. Further detailed studies are warranted to decipher the complicated interaction between free cytosolic calcium, mutant calmodulin and SK2 subunits.

Clinical Implications

Calmodulin is an important multifunctional Ca²⁺-binding messenger protein that regulates several functions in eukaryotic cells. Calmodulin mutation may be associated with multiple cardiac arrhythmic phenotypes, including LQTS, CPVT and idiopathic VF.²⁸ Enhanced L-type Ca²⁺ current and aberrant ryanodine receptor type 2 regulation are among the dominant mechanisms responsible for cardiac arrhythmogenesis.^{29, 30} Prior studies showed that SK currents are upregulated in pathogenic conditions while SK current blockade may be

proarrhythmic,^{10, 31} suggesting that SK current upregulation is a physiological response to reduced repolarization reserve and that SK current blockade might be arrhythmogenic in certain clinical conditions.³² The data obtained in our present study suggest that mutant calmodulin impedes the activation of SK current, which may play a role in the arrhythmic phenotypes experienced by patients with calmodulin mutations. However, despite dramatic differences in both Ca²⁺ affinity and clinical phenotypes (LQTS, CPVT and idiopathic VF), all mutations had similar effects on SK current density in HEK cells. Therefore, further studies are needed to confirm the relevance between the present study and calmodulinopathy.

Limitations

In this study we used ATX-II to create an in vitro model of LQTS³³ and showed that apamin administration potentiated APD prolongation. These results are relevant only to LQTS. Whether or not SK current is relevant to CPVT or idiopathic VF remains unclear. Li et al³⁴ recently demonstrated that mutation of the N-lobe not only reduced Ca²⁺ affinity but also disrupted the constitutive interaction between calmodulin and SK channels, leading to rapid dissociation of mutant calmodulin from the SK channel complex. In the in vitro affinity study, N54I did not lose its Ca²⁺ affinity on either C-lobe or N-lobe.²⁷ These findings suggest that the mechanisms by which N54I impedes SK2 current activation might be different than that of D96V. Therefore, the results of the D96V studies may not be applicable to other calmodulin mutations. The exploration of detailed molecular interaction between SK2 channel and mutant calmodulin and the mechanism through which the regulation of SK current is impaired by mutant calmodulin is limited by the unavailability of calmodulin antibodies that can distinguish the WT- and mutant calmodulin at this moment and therefore is beyond the scope of the current study.

Conclusion

We conclude that human arrhythmogenic calmodulin mutations impede the activation of SK2 channels in HEK 293 cells. The relevance of these results to calmodulinopathy remains unclear and deserves further study.

Supplementary Material

Refer to Web version on PubMed Central for supplementary material.

Acknowledgements

We thank Jian Tan and Glen Schmeisser for their technical assistance.

Funding Sources: NIH Grants P01 HL78931, R01 HL71140, R41HL124741, R01 HL083374, a Medtronic-Zipes Endowment of the Indiana University, the Indiana University Health-Indiana University School of Medicine Strategic Research Initiative.

References

1. Adelman JP, Maylie J, Sah P. Small-conductance Ca²⁺-activated K⁺ channels: form and function. *Annu Rev Physiol.* 2012; 74:245–269. [PubMed: 21942705]

2. Allen D, Bond CT, Lujan R, Ballesteros-Merino C, Lin MT, Wang K, Klett N, Watanabe M, Shigemoto R, Stackman RW Jr, Maylie J, Adelman JP. The SK2-long isoform directs synaptic localization and function of SK2-containing channels. *Nat Neurosci.* 2011; 14:744–749. [PubMed: 21602822]
3. Xu Y, Tuteja D, Zhang Z, et al. Molecular identification and functional roles of a Ca(2+)-activated K⁺ channel in human and mouse hearts. *J Biol Chem.* 2003; 278:49085–49094. [PubMed: 13679367]
4. Qi XY, Diness JG, Brundel BJ, Zhou XB, Naud P, Wu CT, Huang H, Harada M, Aflaki M, Dobrev D, Grunnet M, Nattel S. Role of small-conductance calcium-activated potassium channels in atrial electrophysiology and fibrillation in the dog. *Circulation.* 2014; 129:430–440. [PubMed: 24190961]
5. Zhang Q, Timofeyev V, Lu L, Li N, Singapuri A, Long MK, Bond CT, Adelman JP, Chiamvimonvat N. Functional roles of a Ca²⁺-activated K⁺ channel in atrioventricular nodes. *Circ Res.* 2008; 102:465–471. [PubMed: 18096820]
6. Chua SK, Chang PC, Maruyama M, et al. Small-conductance calcium-activated potassium channel and recurrent ventricular fibrillation in failing rabbit ventricles. *Circ Res.* 2011; 108:971–979. [PubMed: 21350217]
7. Chang PC, Turker I, Lopshire JC, Masroor S, Nguyen BL, Tao W, Rubart M, Chen PS, Chen Z, Ai T. Heterogeneous upregulation of apamin-sensitive potassium currents in failing human ventricles. *J Am Heart Assoc.* 2013; 2:e004713. [PubMed: 23525437]
8. Lee YS, Chang PC, Hsueh CH, Maruyama M, Park HW, Rhee KS, Hsieh YC, Shen C, Weiss JN, Chen Z, Lin SF, Chen PS. Apamin-Sensitive Calcium-Activated Potassium Currents in Rabbit Ventricles with Chronic Myocardial Infarction. *J Cardiovasc Electrophysiol.* 2013
9. Nagy N, Szuts V, Horvath Z, et al. Does small-conductance calcium-activated potassium channel contribute to cardiac repolarization? *J Mol Cell Cardiol.* 2009; 47:656–663. [PubMed: 19632238]
10. Chang PC, Hsieh YC, Hsueh CH, Weiss JN, Lin SF, Chen PS. Apamin Induces Early Afterdepolarizations and Torsades de Pointes Ventricular Arrhythmia From Failing Rabbit Ventricles Exhibiting Secondary Rises in Intracellular Calcium. *Heart Rhythm.* 2013; 10:1516–1524. [PubMed: 23835258]
11. Yu CC, Ai T, Weiss JN, Chen PS. Apamin does not inhibit human cardiac Na⁺ current, L-type Ca²⁺ current or other major K⁺ currents. *PLoS One.* 2014; 9:e96691. [PubMed: 24798465]
12. Nyegaard M, Overgaard MT, Sondergaard MT, et al. Mutations in calmodulin cause ventricular tachycardia and sudden cardiac death. *Am J Hum Genet.* 2012; 91:703–712. [PubMed: 23040497]
13. Crotti L, Johnson CN, Graf E, et al. Calmodulin mutations associated with recurrent cardiac arrest in infants. *Circulation.* 2013; 127:1009–1017. [PubMed: 23388215]
14. Marsman RF, Barc J, Beekman L, Alders M, Dooijes D, van den Wijngaard A, Ratbi I, Sefiani A, Bhuiyan ZA, Wilde AA, Bezzina CR. A mutation in CALM1 encoding calmodulin in familial idiopathic ventricular fibrillation in childhood and adolescence. *J Am Coll Cardiol.* 2014; 63:259–266. [PubMed: 24076290]
15. Studenik CR, Zhou Z, January CT. Differences in action potential and early afterdepolarization properties in LQT2 and LQT3 models of long QT syndrome. *Br J Pharmacol.* 2001; 132:85–92. [PubMed: 11156564]
16. Wu J, Cheng L, Lammers WJ, Wu L, Wang X, Shryock JC, Belardinelli L, Lei M. Sinus node dysfunction in ATX-II-induced in-vitro murine model of long QT3 syndrome and rescue effect of ranolazine. *Prog Biophys Mol Biol.* 2008; 98:198–207. [PubMed: 19351514]
17. Persechini A, Cronk B. The relationship between the free concentrations of Ca²⁺ and Ca²⁺-calmodulin in intact cells. *J Biol Chem.* 1999; 274:6827–6830. [PubMed: 10066733]
18. Black DJ, Tran QK, Persechini A. Monitoring the total available calmodulin concentration in intact cells over the physiological range in free Ca²⁺ Cell Calcium. 2004; 35:415–425. [PubMed: 15003851]
19. Maier LS, Ziolo MT, Bossuyt J, Persechini A, Mestral R, Bers DM. Dynamic changes in free Ca-calmodulin levels in adult cardiac myocytes. *J Mol Cell Cardiol.* 2006; 41:451–458. [PubMed: 16765983]
20. Wu X, Bers DM. Free and bound intracellular calmodulin measurements in cardiac myocytes. *Cell Calcium.* 2007; 41:353–364. [PubMed: 16999996]

21. Saucerman JJ, Bers DM. Calmodulin binding proteins provide domains of local Ca²⁺ signaling in cardiac myocytes. *J Mol Cell Cardiol.* 2012; 52:312–316. [PubMed: 21708171]
22. Xia XM, Fakler B, Rivard A, Wayman G, Johnson-Pais T, Keen JE, Ishii T, Hirschberg B, Bond CT, Lutsenko S, Maylie J, Adelman JP. Mechanism of calcium gating in small-conductance calcium-activated potassium channels. *Nature.* 1998; 395:503–507. [PubMed: 9774106]
23. Schumacher MA, Rivard AF, Bachinger HP, Adelman JP. Structure of the gating domain of a Ca²⁺-activated K⁺ channel complexed with Ca²⁺/calmodulin. *Nature.* 2001; 410:1120–1124. [PubMed: 11323678]
24. Lee WS, Ngo-Anh TJ, Bruening-Wright A, Maylie J, Adelman JP. Small conductance Ca²⁺-activated K⁺ channels and calmodulin: cell surface expression and gating. *J Biol Chem.* 2003; 278:25940–25946. [PubMed: 12734181]
25. Wissmann R, Bildl W, Neumann H, Rivard AF, Klocker N, Weitz D, Schulte U, Adelman JP, Bentrop D, Fakler B. A helical region in the C terminus of small-conductance Ca²⁺-activated K⁺ channels controls assembly with apo-calmodulin. *J Biol Chem.* 2002; 277:4558–4564. [PubMed: 11723128]
26. Keen JE, Khawaled R, Farrens DL, Neelands T, Rivard A, Bond CT, Janowsky A, Fakler B, Adelman JP, Maylie J. Domains responsible for constitutive and Ca(2+)-dependent interactions between calmodulin and small conductance Ca(2+)-activated potassium channels. *J Neurosci.* 1999; 19:8830–8838. [PubMed: 10516302]
27. Hwang HS, Nitu FR, Yang Y, et al. Divergent regulation of ryanodine receptor 2 calcium release channels by arrhythmogenic human calmodulin missense mutants. *Circ Res.* 2014; 114:1114–1124. [PubMed: 24563457]
28. George AL Jr. Calmodulinopathy: a genetic trilogy. *Heart Rhythm.* 2015; 12:423–424. [PubMed: 25460856]
29. Limpitikul WB, Dick IE, Joshi-Mukherjee R, Overgaard MT, George AL Jr. Yue DT. Calmodulin mutations associated with long QT syndrome prevent inactivation of cardiac L-type Ca(2+) currents and promote proarrhythmic behavior in ventricular myocytes. *J Mol Cell Cardiol.* 2014; 74:115–124. [PubMed: 24816216]
30. Sondergaard MT, Tian X, Liu Y, Wang R, Chazin WJ, Chen SR, Overgaard MT. Arrhythmogenic Calmodulin Mutations Affect the Activation and Termination of Cardiac Ryanodine Receptor-mediated Ca²⁺ Release. *J Biol Chem.* 2015; 290:26151–26162. [PubMed: 26309258]
31. Tsai WC, Chan YH, Hsueh CH, et al. Small conductance calcium-activated potassium current and the mechanism of atrial arrhythmia in mice with dysfunctional melanocyte-like cells. *Heart Rhythm.* 2016
32. Chang PC, Chen PS. SK channels and ventricular arrhythmias in heart failure. *Trends Cardiovasc Med.* 2015; 25:508–514. [PubMed: 25743622]
33. Kornyejev D, El-Bizri N, Hirakawa R, Nguyen S, Viatchenko-Karpinski S, Yao L, Rajamani S, Belardinelli L. Contribution of the late sodium current to intracellular sodium and calcium overload in rabbit ventricular myocytes treated by anemone toxin. *Am J Physiol Heart Circ Physiol.* 2016; 310:H426–435. [PubMed: 26637557]
34. Li W, Halling DB, Hall AW, Aldrich RW. EF hands at the N-lobe of calmodulin are required for both SK channel gating and stable SK-calmodulin interaction. *J Gen Physiol.* 2009; 134:281–293. [PubMed: 19752189]

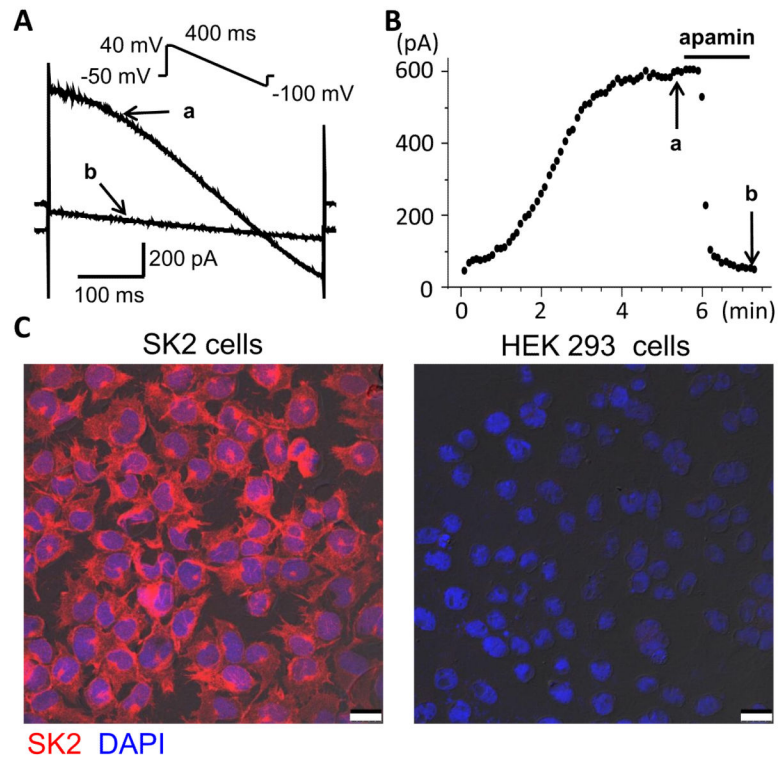


Figure 1. HEK 293 cells that stably express SK2 current. (A) Representative tracings of SK2 currents obtained with ramp protocol shown in the inset at time points indicated by arrow a and b in (B). (B) The time course of SK2 current measured at 0 mV. (C) Immunofluorescence staining for SK2 protein (red) in SK2 cells (left panel) and HEK 293 cells without SK2 (right panel). All cells express SK2 proteins. Blue shows DAPI stain that identifies the nuclei. Scale bar, 25 μm.

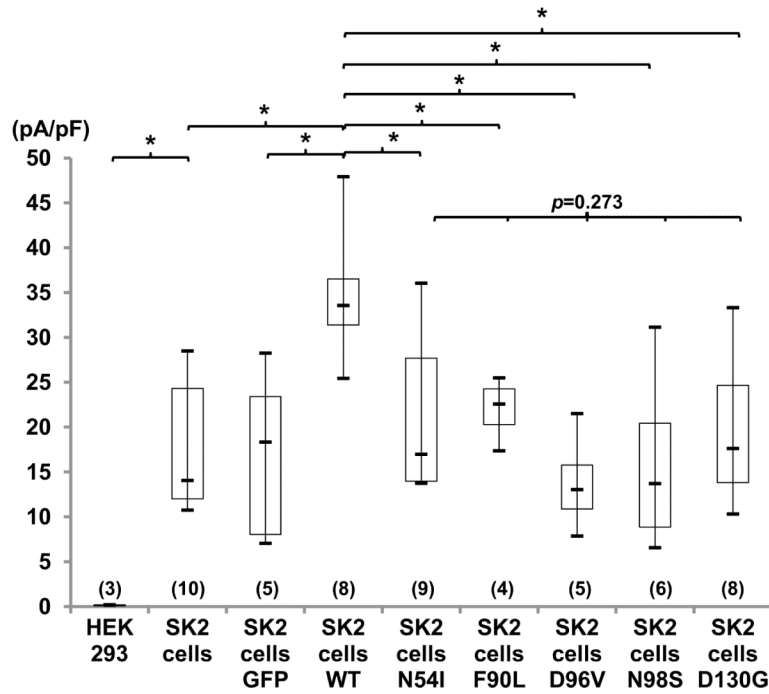


Figure 2. SK2 current densities in HEK 293 cells expressing calmodulin alleles. As compared with SK2 cells, transfection of WT calmodulin significantly increased the current in SK2 cells, while transfection with green fluorescent protein (GFP) or mutant calmodulins failed to increase the current. Numbers in parentheses indicate the number of cells studied. * $p < 0.05$.

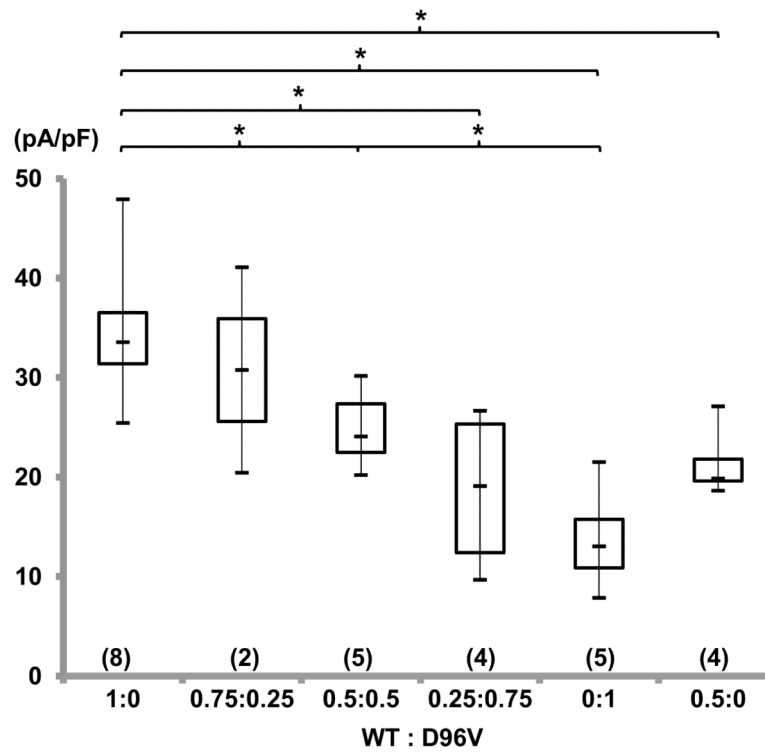


Figure 3. SK2 current densities as a function of WT to D96V ratio. Numbers in parentheses indicate the number of cells studied. SK2 current density was dependent on the amount of WT calmodulin transfected. * $p < 0.05$.

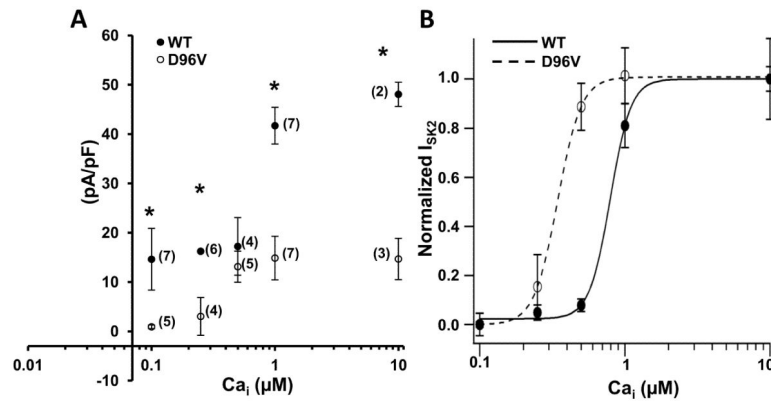


Figure 4. Steady-state calcium dependency of SK2 current transfected with WT- and D96V calmodulins in SK2 cells. (A) SK2 current densities with different intracellular calcium concentrations. (B) SK2 current densities were normalized to the maximal SK2 current with a free calcium of 10 μ M and plotted as a function of calcium concentration. The data were fitted with Hill equation: $y=1/(1+[K_d/x]^n)$, where y indicates the normalized SK2 current and x is the intrapipette free calcium concentration; K_d is the concentration of intrapipette free calcium at half-maximal activation of SK2 current; n is the Hill coefficient. Error bars represent standard error. Numbers in parentheses indicate the number of cells patched. * $p < 0.05$.

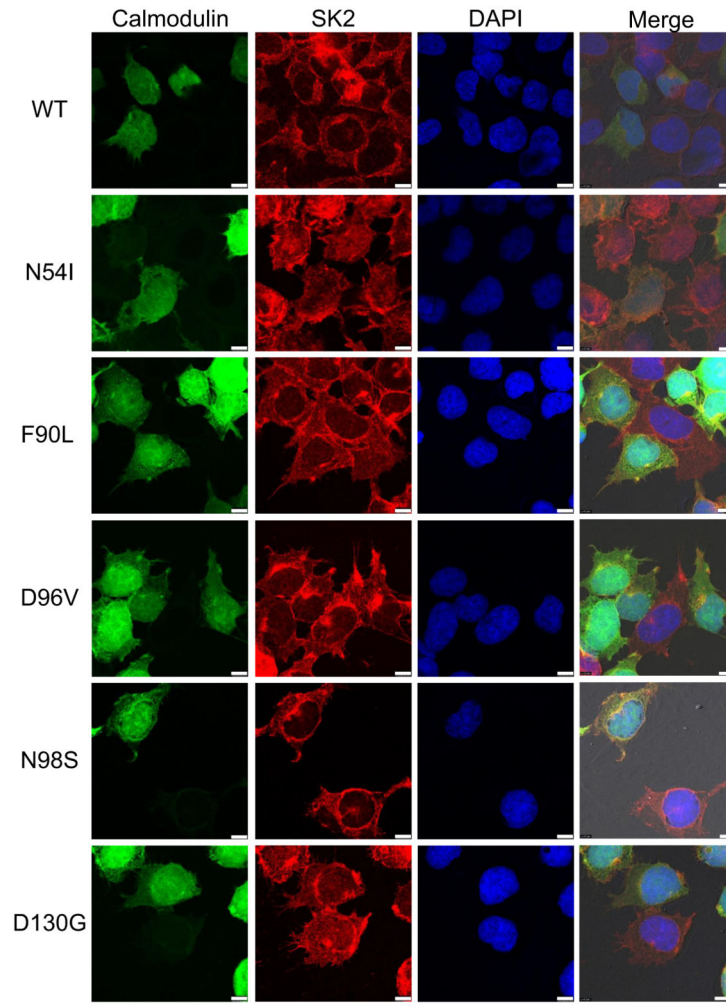


Figure 5. Immunofluorescence of SK2 protein. Cells with and without green fluorescence represent SK2 cells with and without transfected calmodulin, respectively. Red fluorescence shows the staining of SK2 protein. Note that not all cells with SK2 protein express transfected calmodulin. Asterisks were used to label cells without calmodulin transfection. In cells expressing calmodulin, the protein was evenly distributed throughout the cell. Scale bar, 10 μm .

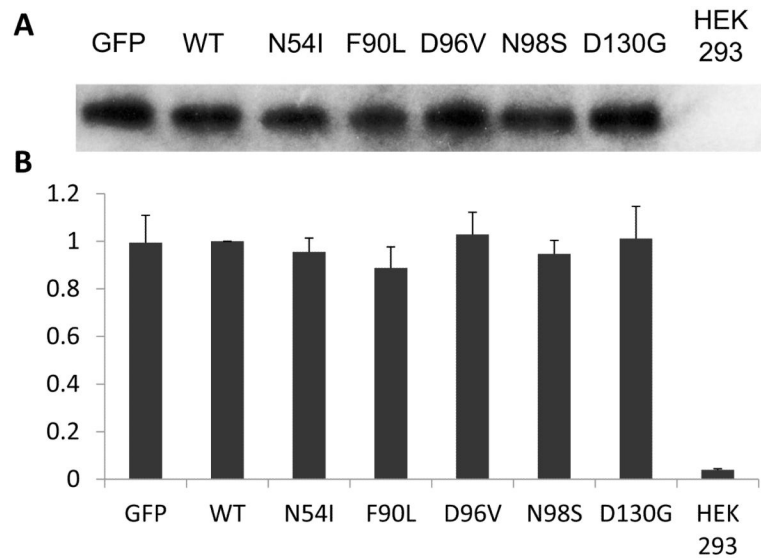


Figure 6. SK2 protein expression in SK2 cells transfected with different types of calmodulin plasmids. (A) A representative immunoblot showing the expression of SK2 proteins in SK2 cells transfected with either WT or mutant calmodulin plasmids (*Top*). (B) A plot showing normalized SK2 protein expression in different types of cells (based on at least 3 experiments).

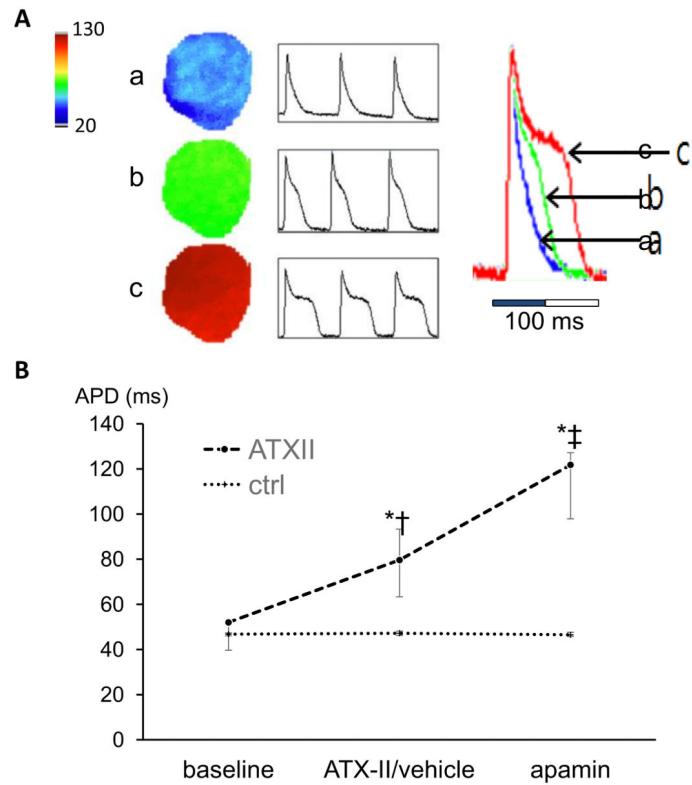


Figure 7. Apamin prolongs APD₈₀ in hearts pretreated with ATXII but not in untreated control (ctrl) hearts. (A) Typical examples of optical action potential at baseline (a), after ATX-II (b) and after apamin (c). (B) A summary of APD changes in 7 ATX-II pretreated and 3 control hearts. Bars indicates ranges from 25% percentile to 75% percentile. * $p < 0.05$ comparing the APD between control and ATXII groups. † $p < 0.005$ comparing the APD between baseline and after ATXII. ‡ $p < 0.005$ comparing the APDs between after ATXII and apamin.